Comparative Medicine
Copyright 2018
by the American Association for Laboratory Animal Science

Vol 68, No 1
February 2018
Pages 63–73

*Original Research*

# Model of Traumatic Spinal Cord Injury for Evaluating Pharmacologic Treatments in Cynomolgus Macaques (*Macaca fasicularis*)

**Nitin Seth,[1] Heather A Simmons,[2] Farah Masood,[1] William A Graham,[3] Douglas L Rosene,[4] Susan V Westmoreland,[5] Sheila M Cummings,[6] Basia Gwardjan,[3] Ervin Sejdic,[7] Amber F Hoggatt,[8] Dane R Schalk,[2] Hussein A Abdullah,[1] John B Sledge,[9] and Shanker Nesathurai[2,3,10,*]**

**Here we present the results of experiments involving cynomolgus macaques, in which a model of traumatic spinal cord injury (TSCI) was created by using a balloon catheter inserted into the epidural space. Prior to the creation of the lesion, we inserted an EMG recording device to facilitate measurement of tail movement and muscle activity before and after TSCI. This model is unique in that the impairment is limited to the tail: the subjects do not experience limb weakness, bladder impairment, or bowel dysfunction. In addition, 4 of the 6 subjects received a combination treatment comprising thyrotropin releasing hormone, selenium, and vitamin E after induction of experimental TSCI. The subjects tolerated the implantation of the recording device and did not experience adverse effects due the medications administered. The EMG data were transformed into a metric of volitional tail moment, which appeared to be valid measure of initial impairment and subsequent natural or treatment-related recovery. The histopathologic assessment demonstrated widespread axon loss at the site of injury and areas cephalad and caudad. Histopathology revealed evidence of continuing inflammation, with macrophage activation. The EMG data did not demonstrate evidence of a statistically significant treatment effect.**

**Abbreviations:** Q, quantitative metric of volitional control; TRH, thyrotropin releasing hormone; TSCI, traumatic spinal cord injury

Traumatic spinal cord injury (TSCI) is a devastating clinical condition.[3,8] The constellation of impairments includes limb weakness, dysesthesias, and bowel, bladder, and sexual dysfunction. Medical and rehabilitation interventions have improved quality of life and long-term survival. Nevertheless, most people treated for TSCI continue to experience residual clinical impairments.

Animal models are important in biomedical research. In the field of TSCI, various species have been used, including mice, rats, cats, dogs, rabbits, and NHP. In these models, the experimental spinal cord injury has been created by diverse methods, some of which require surgical exposure of the spinal cord and lesion induction by using a sharp instrument[7,30,31] or a device that provides static or dynamic compression.[2,4,23] In other models, the dura remains intact, and compression is applied by using a circumferential clip.[34] These approaches are complimentary. However, some pathophysiologic and clinical features of TSCI differ substantially between humans and other species. For example, despite complete anatomic transection, dogs and cats—unlike humans and NHP—may be able to walk.[5,11,12,16] In this context, NHP models have an important role in advancing the understanding of TSCI as well as identifying candidate treatments.

Here we present the results of experiments involving NHP, where the experimental lesions were created by using a balloon catheter that was inserted into the epidural space. Prior to the creation of the lesion, we inserted an EMG recording device to facilitate measurement of tail movement and muscle activity before and after TSCI. This animal model is unique in that the impairment is limited to the tail: the subjects do not experience limb weakness, bladder impairment, or bowel dysfunction. In addition, 4 of the 6 subjects received a combination treatment of thyrotropin releasing hormone (TRH), selenium, and vitamin E after the induction of TSCI.

Two key items in this article are unique. First, we articulate the method by which EMG data from the tail musculature can be used to formulate a quantitative measure of impairment and recovery from TSCI (the Q value). Quantitative measures of impairment and recovery in animal models compliment the subjective measures that focus on observation of limb function or movement. Second, we report the TSCI-associated histopathologic abnormalities present at 90 d after injury. This information is particularly valuable, because few human anatomic specimens at this time point are available, reflecting the epidemiology of human TSCI. Most people with TSCI in developed countries survive for years or decades.[8]

*Received: 07 Jun 2017. Revision requested: 03 Jul 2017. Accepted: 14 Aug 2017.*
*[1]School of Engineering, University of Guelph, Guelph, Ontario, Canada; [2]Wisconsin National Primate Research Center, University of Wisconsin-Madison, Madison, Wisconsin; [3]Division of Physical Medicine and Rehabilitation, Department of Medicine, McMaster University, Hamilton, Ontario, Canada; [4]Department of Anatomy and Neurobiology, Boston University School of Medicine, Boston, Massachusetts; [5]Harvard Medical School, Boston, Massachusetts; [6] Sanofi, Framingham, Massachusetts; [7]Swanson School of Engineering, University of Pittsburgh, Pittsburgh, Pennsylvania; [8]Center of Comparative Medicine, Brigham and Women's Hospital, Boston, Massachusetts; [9]Lafayette Bone and Joint Clinic, Lafayette, Louisiana; and [10]Department of Physical Medicine and Rehabilitation, Hamilton Health Sciences, St Joseph's Hamilton Healthcare, Hamilton, Ontario, Canada*
*[*]Corresponding author. Email: nesathurai@hhsc.ca*

During EMG, data regarding muscle activity are obtained from electrodes placed on the surface of the skin or inserted directly into the muscle groups of interest. In our experiments, we obtained EMG data before and after TSCI by using wire electrodes implanted in the musculature of the tail. Conceptually, the magnitude of EMG signal is related to the amount of muscle activation in the muscle groups. Any individual muscle has a fixed number of motor units, the motor fibers controlled by a single motor neuron, which are the key functional units. These motor neurons are located in the spinal cord and are controlled by neural networks in the spinal cord and brain. In TSCI, limb impairment is attributed, in part, to impaired functioning of these motor units.[24] In these experiments, the number of peaks was obtained from each subject as a feature to develop a Q score. Data collection encompassed the time periods before and after experimental spinal cord injury. Conceptually, this process permits an assessment of impairment and recovery from TSCI and provides an opportunity to evaluate the effect of potential treatments.[18,29]

In these experiments, the candidate treatment comprised TRH, selenium, and vitamin E. In part, the choice of these 3 agents was strategic, because all 3 agents are available for human use. TRH is a tripeptide produced in the hypothalamus; selenium and vitamin E are antioxidants. Compelling evidence in animals indicates that TRH, selenium, and vitamin E modulate recovery in TSCI,[3,14,36,41] and preliminary evidence in humans with TSCI supports the safety and efficacy of TRH.[13,33] Both selenium and vitamin E have been studied in clinical trials involving other disease states and are well tolerated.[1,17,42] However, no animal or human studies have been performed as yet to demonstrate the safety and efficacy of the combination of these 3 agents for the treatment of TSCI.

## Materials and Methods

**Subjects enrolled.** The subjects were healthy, research-naïve, adult male cynomolgus macaques (*Macaca fascicularis*; $n = 6$; weight, 6 to 13 kg), which were free of *Macacine herpesvirus 1*, simian T-lymphotropic virus 1, simian retrovirus type D, and SIV at the time of the study. The first 4 subjects received combination pharmacologic treatment; the remaining 2 subjects did not receive treatment.

**Housing and husbandry.** The subjects were pair-housed in metal cages before surgery but individually housed in a room with other cynomolgus macaques after surgery. The subjects were fed twice daily (Primate Diet, ZuPreem, Shawnee, KS, or Teklad 2050 20% Protein Diet, Envigo, East Millstone, NJ). The housing area was on a 12:12-h light:dark cycle. All macaques received an enrichment program.

**Anesthesia and postsurgical pain management.** All procedures were completed under general anesthesia and with aseptic technique.

Anesthesia induction was achieved by using ketamine (10 to 20 mg/kg IM) and atropine (0.03 to 0.006 mg/kg IM). The hair in the area of the incisions was shaved. The skin was cleansed with alternating applications of surgical scrub and alcohol. An intravenous catheter was inserted, and normal saline or lactated Ringer solution was administered at a rate of 5 to 10 mL/h. Each subject was endotracheally intubated and mechanically ventilated. Anesthesia was maintained with inhaled isoflurane at 1% to 2% minimal alveolar concentration; ECG and oxygen were monitored continuously. Heart rate, blood pressure, temperature, and respiratory rate were closely monitored by the veterinary staff. The surgical sites were appropriately draped.

To manage pain related to the surgical procedures, either buprenorphine (0.005 to 0.03 mg/kg IM every 8 to 12 h) or sustained-release (0.06 to 0.2 mg/kg SC daily) was administered. Additional analgesia was achieved by using meloxicam (0.1 to 0.2 mg/kg PO or SC daily). The initial dose of analgesic medications was administered before surgery. In addition, the margins of the surgical incisions were infiltrated with a 1:1 mixture of lidocaine and marcaine.

**Initial surgical procedure to facilitate the collection of EMG data.** On the lower back of each macaque, a midline incision was placed superior to the proximal tail and a small pocket was dissected between the underlying muscle and subcutaneous fat. Additional small incisions were made on the left and right side of the tail to expose the flexor cauda longus and brevis muscles; these muscles are an agonist–antagonist pair. A small telemetry device (Data Sciences International, Minneapolis, MN) was inserted into the pocket in the lower back. The telemetry device is attached through a set of wire electrodes, which were implanted into the left and right flexor cauda longus and brevis. The exposed areas of the electrodes were 10 mm; the distance between the active and reference electrodes was 5 mm. Figure 1 illustrates this experimental approach.

The tail of cynomolgus macaques can be considered a fifth limb, which is involved in the performance of functional tasks and balance.[19,32,35] The tail has well-developed sensory and motor areas. EMG data were collected by radiofrequency link to a computer for 30 d to determine baseline tail movements. Data collection occurred Monday through Friday (excluding holidays) for approximately 1 h daily. The EMG responses were mathematically transformed into a quantitative metric for volitional control of tail movement; we have termed this metric 'Q.' The method by which Q was calculated is described later.

**Subsequent surgical procedure to create experimental spinal cord injury.** At 30 d after implantation of the transmitter, the subjects underwent a second surgery. The anesthesia and postsurgical pain management plan were the same as described earlier.

A small laminotomy was performed at the level of the fifth lumbar vertebra. An epidural balloon catheter was inserted and advanced approximately 10 cm cranial, to the level of the lower thoracic spinal cord. The balloon was inflated rapidly and remained inflated for 1 min. Conceptually, this procedure corresponds to human SCI, in that there is a rapid transfer of energy (that is, initial balloon inflation), followed by residual displacement of tissues such as disk material, boney fragments, or hematoma (that is, continued balloon inflation for 60 s). The balloon was then deflated. The catheter was removed, and the surgical incision was closed.

The radiographic image in Figure 2 highlights the location of the experimental lesion in the low thoracic vertebra. The CT image in Figure 3 demonstrates how the lesion is created and the displacement of the thoracic spinal cord by the epidural catheter. After the lesion was created, the subject remained anesthetized for 1 h. This time period is a typical duration between injury and the availability of emergency medical treatment in humans.

After 1 h, 4 macaques (treatment group) received an intravenous bolus of TRH (dose, 0.2 mg/kg) followed by continuous intravenous infusion for 1 h of selenium (60 mg, 0.2 mg/kg/h). In addition, vitamin E (dose, 80 IU) was administered orally once daily starting 1 d after surgery and continuing for 90 d. In addition, 2 macaques (untreated control group) received an infusion of normal saline for 1 h. These control subjects did not receive any selenium or vitamin E. All the subjects experienced a spinal cord lesion.

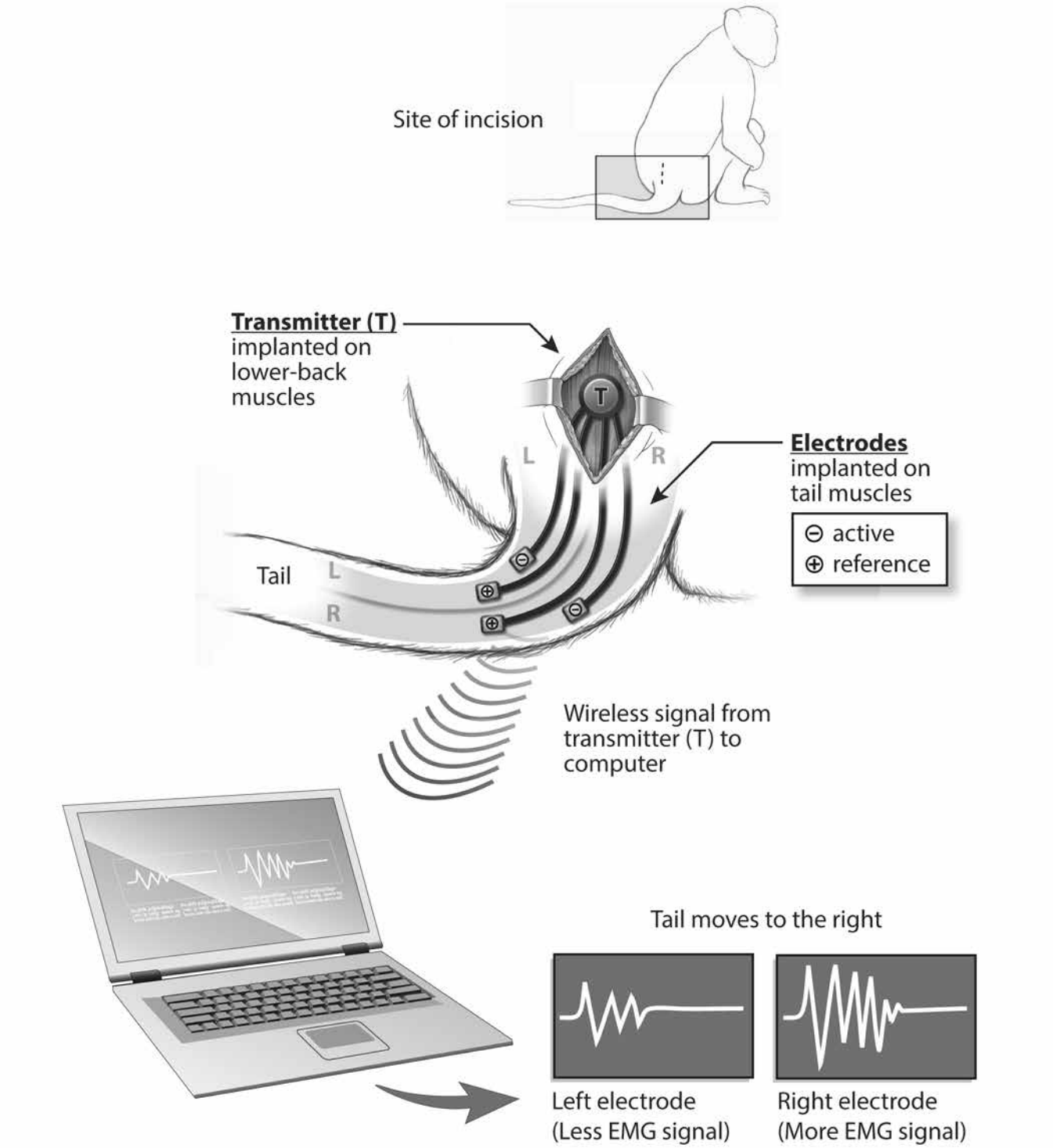


**Figure 1.** The transmitter to collect EMG data is surgically implanted in the macaque's lower back and connected to recording wire electrodes in the flexor cauda longus and brevis of the tail. The EMG data are transmitted by a radiofrequency link to a computer. Adapted and modified from reference[28].

In 5 subjects (4 with treatment, and 1 without treatment), EMG data were recorded from day 0 (day of creation of the selective lesion) through day 90. In the remaining (untreated) subject, EMG data were obtained for 120 d after TSCI.

**Monitoring of subjects.** The investigators and veterinary staff closely monitored all subjects. The frequency of assessment was at least twice daily and was more frequent during the immediate postsurgical periods. The macaques were assessed monitored for clinical indicators of illness including limb weakness, vomiting, diarrhea, jaundice, bleeding, and anorexia. Animals were weighed at the time of a surgical procedure, and prior to euthanasia. The subjects were monitored for wasting and emaciation, as clinical indicators of weight loss.

**Euthanasia and postmortem examination.** On day 90, 5 of the subjects were euthanized by sedation with ketamine (10 to 20 mg/kg IM) followed by sodium pentobarbital (>50 mg/kg IV); the remaining subject (untreated control) was euthanized at 120 d after creation of the spinal cord lesion. The postmortem

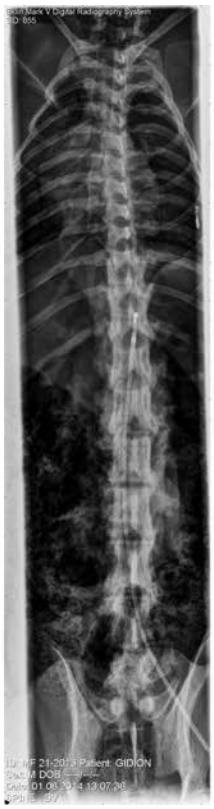

**Figure 2.** Standard radiograph of catheter inserted into the epidural space via laminotomy in a cadaveric subject. The balloon is not inflated in this image.

examination was performed immediately after euthanasia. The gross and microscopic examination included assessment of the brain, spinal cord, heart, liver, spleen, kidneys, and bladder. Venous blood was obtained immediately prior to euthanasia; cerebrospinal fluid was obtained also.

The research involving the first 2 subjects was completed at the New England Primate Research Center, where the animals were cared for in accordance with the National Research Council's *Guide for the Care and Use of Laboratory Animals* (8th edition)[20] and the standards of the Harvard Medical School Standing Committee on Animals. Research on the remaining 4 subjects was completed at the Wisconsin National Primate Research Center and was approved by the IACUC at the University of Wisconsin at Madison. The macaques were under close supervision by the veterinary staff and were monitored for any adverse effects.

**Histopathologic assessment.** For histopathology, tissue blocks were dissected from the epicenter of the lesion and sites caudal and cephalad. These blocks were fixed in 10% neutral buffered formalin for 7 d, embedded in paraffin, and cut at 5 µm. Standard hematoxylin and eosin staining was done on sections from all blocks. In addition, sample sections were stained with Luxol fast blue to highlight myelin changes.

Standard immunoperoxidase immunohistochemistry for ionized calcium binding adapter molecule 1 (Iba1), a macrophage-e and microglia-specific marker, was performed also. Sections of brain and spinal cord were deparaffinized, rehydrated, and blocked with 3% hydrogen peroxide in PBS. Iba1 pretreatment involved microwaving for 20 min in 0.01 M sodium citrate buffer, followed by 20 min of cooling. After pretreatment, avidin–biotin blocking (Invitrogen, Frederick, MD) and protein blocking (10 min; Dako, Carpinteria, CA) were

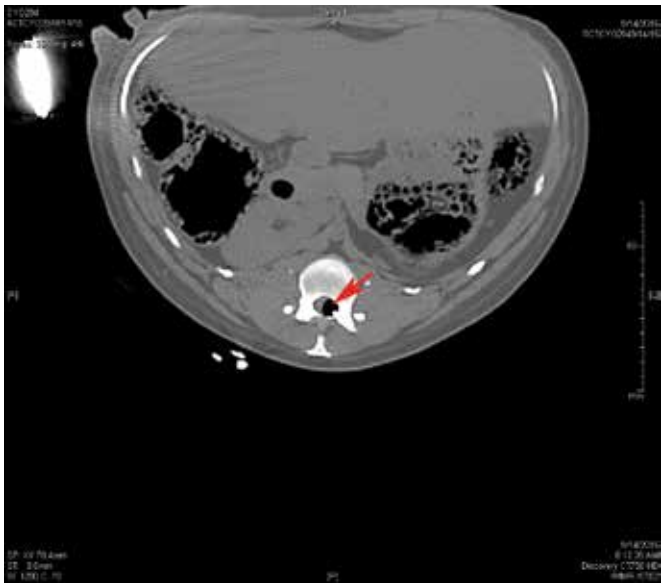

**Figure 3.** CT image of the inflated balloon in the epidural space of the thoracic spine. The balloon is inflated with air, which appears black in the spinal column (red arrow). Note that 60% of the column is occupied by the balloon, and the spinal cord is displaced. This image is from a cadaveric subject.

conducted on all sections. A wash of Tris-buffered saline followed each step.

**Analysis of EMG data.** Conceptually, the overriding goal was to convert the raw unprocessed longitudinal EMG data into a metric of volitional tail movement (that is, Q). The collection and analysis of EMG data of this nature is novel. Specifically, this data set contains longitudinal EMG data from the tail musculature. Furthermore, the muscles are an agonist–antagonist pair. The availability of prelesion and postlesion data is particularly valuable. In this context, no prescriptive or established analysis paradigms are available.

The statistical power in these experiments in enhanced by the collection of prelesion and postlesion EMG data. This inclusion permits the normalization of the postlesion data for each subject, and theoretically, decreases statistical variances. In addition, the prelesion and postlesion data were collected daily, and each recording date serves as a unique data point. This feature facilitates inferences related to the trajectory of recovery. In total, the data set contains approximately 800 million distinct observations. Consequently, this experimental strategy decreases the number of subjects required to ascertain a treatment effect.

Of note, the data from the first subject were used to formulate a preliminary analysis paradigm.[37] This preliminary study focused on analyzing the number of turns and the area under the EMG waveform. The determination of Q in the current study is substantively different from the previously articulated analysis strategy. In particular, here we calculated Q according to the number of peaks in the EMG data, which is a different EMG parameter that was used in the previous preliminary analysis. In addition, the current EMG data were processed with signal rectification, thresholding, and smoothing, as methods to emphasize times of high activity from nearby motor units, an aspect not used previously studied. Furthermore, the analysis is based on the entire study population.

In calculating Q, the EMG data were processed based on the following fundamental assumptions:

1. The lesion perturbs the EMG signal that was collected from the tail musculature.

2. The wire electrodes detect all electrical EMG activity from all the motor units 'close' to the electrodes. Because motor units contain motor fibers, the EMG activity also represents the EMG activity of all the motor fibers as well.
3. Insertion of the wire into the muscle initially may disrupt the tissue, causing associated inflammation that may affect signal variability initially; this variability decreases as inflammation subsides. Therefore, the wire–tissue interface 'matures' over time after initial implantation and produces more reliable signals. Consequently, the EMG signal later in the recording period is less likely to be affected by artifact related to surgical implantation.
4. The number of peaks in the aggregate EMG signal acts as a surrogate of motor unit (MU) activation. From a clinical perspective, this activation translates into greater tail movement.

The following steps summarize the signal processing strategy:

1. Filtering: Wavelet denoising is performed to eliminate 'noise.' The objective of filtering is to retain as much of the original signal while attenuating noise.[7,37]
2. Rectification: After filtering, the signals are rectified to convert all the negative values to positive values. This process resolves positive–negative signal cancellation.
3. Smoothing: A moving average is calculated for a continuous segment containing 10,000 data points. This information is used to mathematically 'smooth' the rectified EMG signals and reduce the effect of artifacts.
4. Thresholding: The spikes with low amplitude are discarded. This step ensures that data from the motor units close to the electrode are imputed in the calculation of Q.

As a result of the signal processing strategy, the total number of peaks per daily recording session were calculated. This value was reduced by the average (arithmetic mean) number of peaks for each prelesion day (that is, after insertion of transmitter but before creation of the spinal cord lesion). Finally, this number was divided by the standard deviation of the number of peaks in the prelesion period. This approach 'normalized' raw data relative to the activity in the prelesion period.

As such, for every day of EMG recording, a value of Q was calculated. The values of Q were calculated separately for muscles of the left and right sides of the tail. To determine whether tail movement before the lesion differed from that afterward and to ascertain whether combination therapy had an effect, a linear regression model was used.

The first effect tested by using the model relates to the EMG consequences of the lesion. Stated more explicitly, did the lesion cause a change in Q? The second effect tested relates to whether combination treatment resulted in improved Q scores when compared with the absence of treatment. In other words, was combination treatment effective?

Due to the longitudinal nature of the study, the rates of each effect were tested. When the effects were not significant ($P > 0.05$), they were subsequently removed from the model. Data from the right and left tail muscles were tested separately. The analyses were conducted by using SAS 9.1 (SAS Institute, Cary, NC) and MatLab (Mathworks, Natick, MA).

## Results

**Animal welfare related to experimental protocol and administration of combination treatment.** The macaques were closely monitored by the investigators, veterinarians, and animal research technicians for indicators of illness including limb weakness, vomiting, diarrhea, jaundice, bleeding, and anorexia. All 6 subjects tolerated implantation of the telemetry device and did not explant the device. None of the subjects required pain medications beyond the immediate 72-h time postsurgical time frame. The macaques did not traumatize their tails or engage in behaviors indicative with pain. Consistent with the experimental goals, there was no evidence of limb weakness or bowel or bladder dysfunction. The subjects were monitored for weight loss, and there were no abnormalities.

The infusion of TRH is potentially associated with cardiac arrhythmias. In this protocol, the medication was administered while the subject was under anesthesia and had continuous ECG monitoring. No arrhythmias were identified in the treated or untreated subjects.

Blood samples were obtained immediately prior to euthanasia, with necropsy examinations performed immediately thereafter. Gross and microscopic examinations included assessment of all major organs. The postmortem examination was focused on evaluation of the brain, spinal cord, and potential systemic complications related to TSCI. For example, subjects with spinal cord injury can experience autonomic dysreflexia, which could result in hypertension, which may result in stroke and cardiac hypertrophy.[27] Alternatively, TSCI can result in detrusor sphincter dyssnergia, which can be associated with postmortem features of hydronephrosis and bladder hypertrophy.[27] None of the subjects demonstrated evidence of pathology beyond the spinal cord. Furthermore, laboratory indices, including CBC, liver function tests, and prothrombin times, did not demonstrate abnormalities that could be potentially attributed to toxicity of selenium or vitamin E. These finding provides further reassurance regarding animal welfare issues.

**Histopathologic features.** On gross examination, no significant abnormalities were noted, particularly of the vertebrae, dura, and substance of the spinal cord. The site of laminectomy was healed and showed both osseous and periosteal regeneration.

Microscopic evaluation of fixed tissues specimens was similar in all subjects. Dilated myelin sheaths (diameter, ≤75 µm) were present multifocally within the white matter funiculi. The axons were either swollen (spheroids) or had been replaced by phagocytic microglia (Wallerian degeneration). Areas of vacuolization (spongiosis) and collections of microglial cells (glial nodules) were present in both the gray and white matter. These findings were noted at the epicenter of the lesion as well as cephalad and caudal to the lesion.

At the site of injury, neurons in gray matter were often surrounded by more than 4 glial cells (satellitosis). Many neurons were swollen, with a loss of Nissl substance and cellular detail (chromatolysis). The nuclei were often faded with dispersed chromatin (degeneration). Representative microscopic images are shown in Figures 4 through 8 . Qualitative histopathologic features were similar in all 6 subjects. The descriptions of the histopathologic features represent the consensus of 3 veterinary pathologists.

**EMG features.** Although data were collected from all 6 macaque, information from one side of one macaque was not stored. As such, the analysis of the EMG data represents the experience of 3 subjects who received combination treatment and 2 subjects who did not (untreated controls).

Table 1 summarizes the Q values at key time points, and Figure 9 represents a fitted linear regression model for the aggregate data of Q before and after creation of the lesion. Consistent with maturation of the wire–muscle interface, the value of Q for both the left and right side of the tail increased during the prelesion period. Immediately after lesion, the value of Q decreased on both the left and right side in both the treatment and control groups. The Q scores before and after creation of the spinal cord lesion are statistically significant (left side, $P = 0.021$; right side, $P = 0.01$). This finding suggests that the lesion led to decreased EMG activity, resulting in

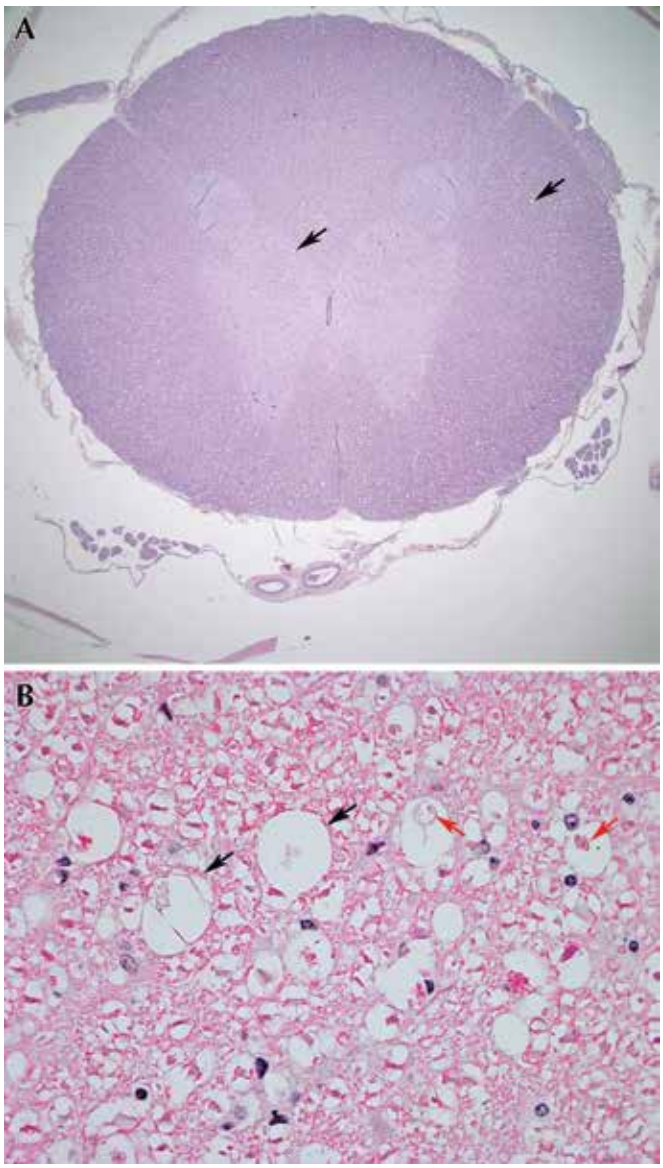


**Figure 4.** (A) Photomicrograph of the spinal cord at the epicenter of the lesion. The gray and white parenchyma are disrupted by dilated myelin sheaths (spongiosis; arrows), which are widespread. These findings are noted caudal and cephalad to the lesion, in both treated and untreated subjects. Hematoxylin and eosin stain; magnification, 40×. (B) Photomicrograph of the spinal cord (white matter funiculi) at epicenter of experimental injury. There are many dilated myelin sheaths (spongiosis; black arrows), some of which contain degenerating or swollen axons (red arrows). These findings are noted caudal and cephalad to the lesion, in both treated and untreated subjects. Haematoxylin and eosin stain; magnification, 400×.

decreased tail movement, and supports the construct that Q can be used as a measure of impairment after experimental TSCI.

On the left side, the treatment group was associated with a trend toward higher Q-values, when compared with the untreated control group ($P = 0.075$); this effect was not noted on the right side ($P = 0.519$). Fitted Q values (Table 1) increased with time in both groups, although the absolute values on both sides were higher after treatment. Overall, the EMG data are insufficient to impute an effect of treatment.

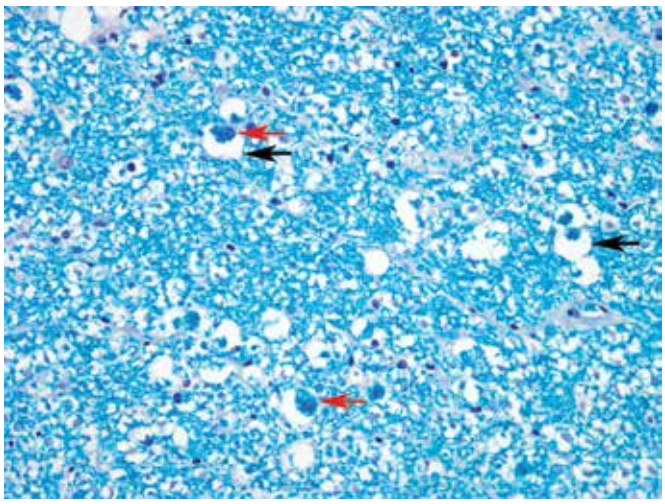

**Figure 5.** Photomicrograph of the spinal cord cranial to epicenter of the spinal cord lesion. Dilated myelin sheaths (black arrows) and swollen axons (spheroids; red arrows) are present. Luxol fast blue stain; magnification, 400×.

## Discussion

In these experiments, spinal cord injury was created by using a balloon catheter placed in the epidural space of cynomolgus macaques. The initial inflation of the balloon in the macaque model corresponds to the initial transmission of energy in human TSCI. Maintaining the balloon inflated corresponds to pressure on the spinal cord from structures such as disk material, bone fragments, and hematoma in humans. The lesions in the macaques were created without compromising the dura, consistent with most human TSCI. Specifically, the model has no tearing or laceration of the dura, with no leakage of cerebral spinal fluid.[38] As previously reported, lesions created by this method have the same histopathologic features of human spinal cord injury during the acute phase (that is, 1 h after injury).[18]

There are few histopathologic studies of human TSCI at 3 mo after injury, reflecting the epidemiology of the disease. In particular, most people with TSCI in developed countries survive for years or decades. Consequently, anatomic tissues from patients who died within 3 mo of TSCI are sparse. In this context, the data from our NHP subjects are particularly valuable.

In addition, the histopathologic features associated with the lesions created by this method are similar to human TSCI during the subacute phase (that is, at 90 d after injury).[28] Human TSCI, at this time point, is characterized by axonal loss, demyelination, and microglial activation, consistent with experimental results in NHP.[6,9,15] Conceptually, this model is most relevant to TSCI at the thoracic level rather than cervical TSCI.

From a histopathologic perspective, TSCI can be classified as concussions, contusions, lacerations, and solid cord injuries.[6,22] Concussions are typically associated with transient neurologic complaint, with no identifiable pathologic challenges. Lacerations are the result of penetrating injuries, such as those caused by knife or bullet wounds. Contusions are associated with violent nonpenetrating injuries, with substantive disruption of spinal cord architecture. Solid-core lesions are associated without gross disruption of the spinal cord architecture. The lesions created in the current experiments are most consistent with solid-core lesions.

In severe human TSCI, there is an epicenter of substantive disruption, with a characteristic perimeter of less-injured spinal cord structures.[22] Our NHP model may be particularly relevant to understanding these less-injured structures, which might be

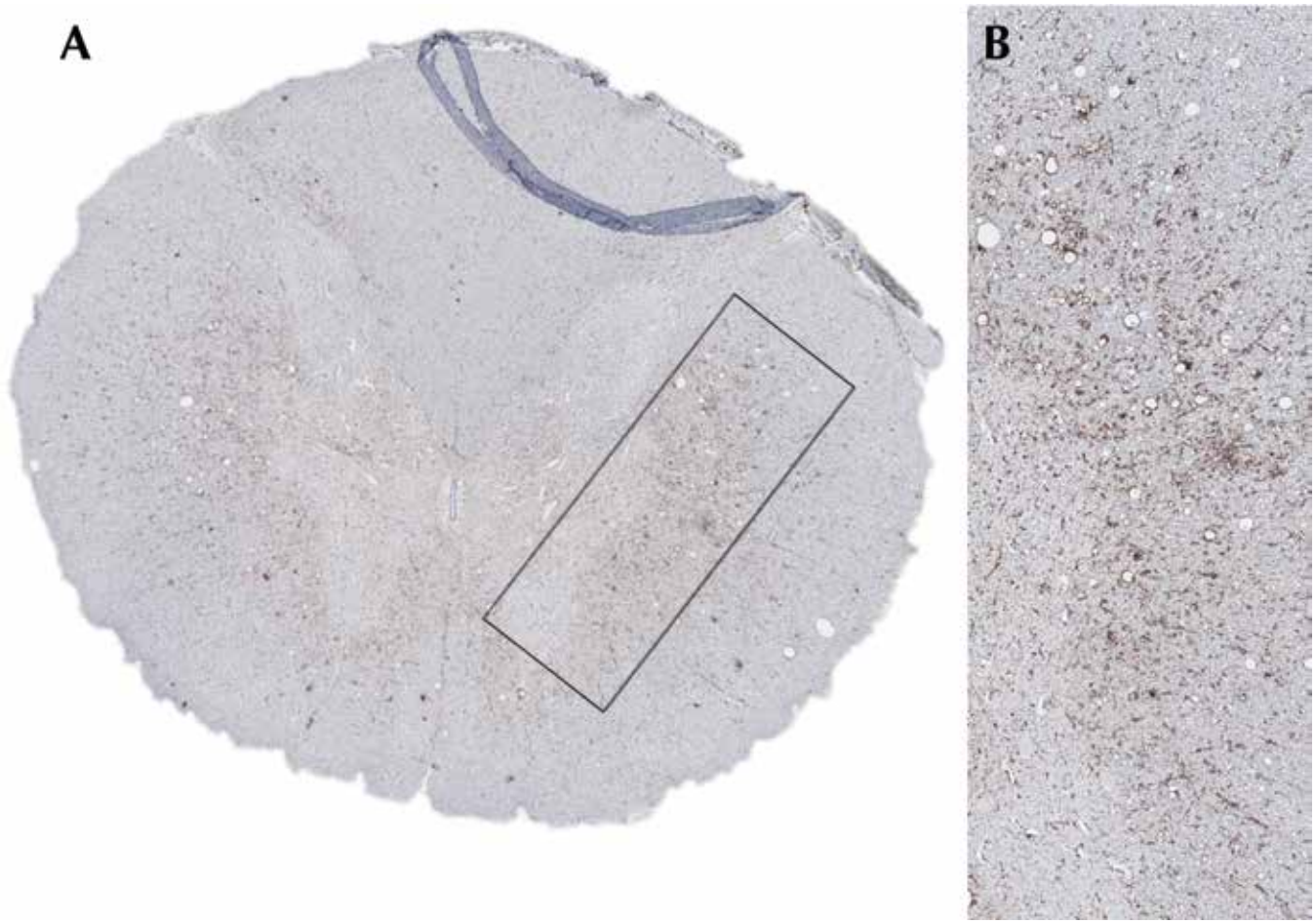


**Figure 6.** (A) Photomicrograph of the spinal cord at the epicenter of experimental lesion. Reactivity to Iba1 is present within the white matter adjacent to the gray matter with spongiosis of the parenchyma; magnification, 40×. (B) Increased magnification of region denoted by the box in A. These findings suggest that substantial inflammation continues at the 90-d time point. Iba1 immunohistochemistry with DAB staining and counterstained with hematoxylin; 400x magnification.

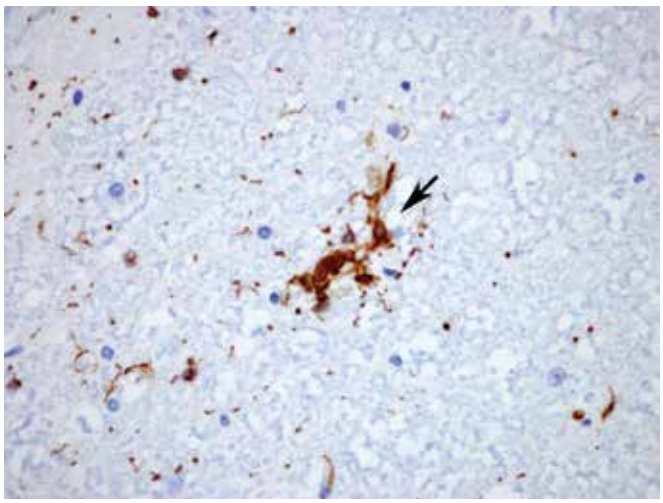

**Figure 7.** Photomicrograph of the spinal cord gray matter at the epicenter of experimental lesion. This figure shows Iba1-positive cells at the level of the lesion. These microglia show the hypertrophic phenotype typical of activated microglia Iba1 immunohistochemistry with DAB staining and counterstained with hematoxylin. Magnification, 400×.

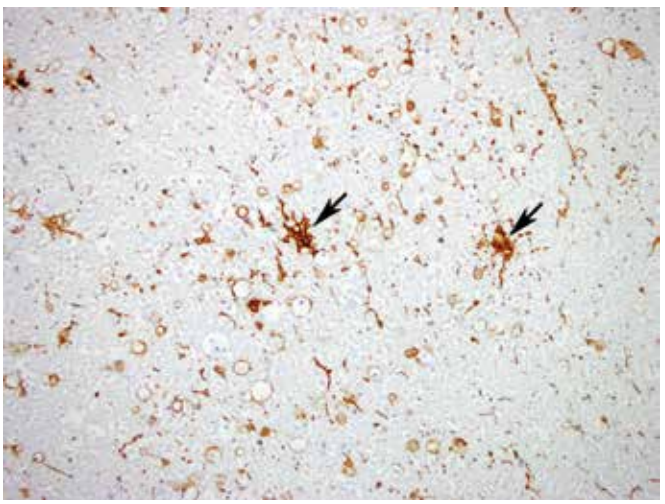

**Figure 8.** Photomicrograph of the spinal cord cephalad to epicenter of spinal cord lesion. Immunohistochemistry using Iba1 antibody highlights microglial cells. Microglial cells (black arrows) demonstrate an activated phenotype (that is, thickened processes, enlarged cell body). Iba1 immunohistochemistry with DAB staining and counterstained with hematoxylin. Magnification, 200×.

more amenable to pharmacologic treatment than the injured tissue at the epicenter. Furthermore, our macaque subjects had histopathologically substantive, widespread axonal loss, despite a relatively focused lesion in the thoracic spinal cord. We speculate that proinflammatory chemical mediators might be generated at the epicenter of the lesion and subsequently be

**Table 1.** Standardized Q scores

| | Subject | Day of implantation | Prelesion, midpoint | Postlesion, day 1 | Postlesion, midpoint | Study end |
|---|---|---|---|---|---|---|
| Right side | 1 | 0.548 | 0.693 | 0.016 | 0.322 | 0.645 |
| | 2 | 0.553 | 0.696 | 0.016 | 0.320 | 0.639 |
| | 3 | 0.552 | 0.696 | 0.016 | 0.320 | 0.641 |
| | 4 | 0.604 | 0.731 | 0.014 | 0.283 | 0.566 |
| | 5 | 0.585 | 0.719 | 0.015 | 0.296 | 0.591 |
| Left side | | | | | | |
| | 1 | 0.855 | 0.902 | 0.005 | 0.103 | 0.207 |
| | 2 | 0.695 | 0.793 | 0.011 | 0.217 | 0.435 |
| | 3 | 0.798 | 0.863 | 0.007 | 0.144 | 0.288 |
| | 4 | 0.836 | 0.888 | 0.006 | 0.117 | 0.235 |
| | 5 | 0.948 | 0.965 | 0.002 | 0.037 | 0.073 |

Q scores for each subject increase after the time of insertion and reach a plateau during the prelesion period. This pattern reflects maturation of the wire–muscle interface. The Q score decreases immediately after creation of the lesion and gradually increases (improves) over time. The values of Q relative to time are nonlinear.

disseminated to other parts of the spinal cord due to its rich and redundant vascular supply.

Of note, despite the extensive histopathologic findings, our subjects did not have any clinical impairment such as limb weakness, bowel impairment, or bladder dysfunction. This clinical picture is in the context of clear neurophysiologic evidence of impairment in the tail musculature, thus suggesting that the resiliency or redundancy of the spinal cord may be greater than has previously been appreciated. Alternatively, the lack of clinical impairment, despite substantive histopathologic abnormalities, may imply the importance of residual displacement or compression of the spinal cord (that is, because of herniated disk material, disruption of the architecture of the spinal column due to fracture or dislocation, and so forth) in continued clinical impairment. Limb weakness might have been induced in our macaques by using a larger balloon or increasing the time that the balloon remained inflated (or both). However, that approach would have been adverse to animal welfare and might preclude long-term survival of the subjects.

Demonstrating the efficacy of animal models of TSCI is more challenging than determining their safety. Safety can be ascertained readily through close surveillance of clinical abnormalities and detailed review of laboratory and necropsy findings. Inferences related to efficacy in humans require the identification of animal behaviors that correspond to human function. In human TSCI, the primary goal of treatment is to improve limb control for performing functional tasks (that is, walking, dressing, feeding, bathing, and so forth). As evidenced by EMG data, functioning motor units are essential to limb movement, which is essential to attaining greater independence in functional tasks.[24] In this context, the EMG endpoint in our model is a meaningful measure of impairment and recovery. Furthermore, different levels of neurologic recovery are required for different functional tasks. In humans with TSCI, we consider that weight-bearing in the lower extremities and walking requires a lower level of recovery of motor control than that required for manipulating objects by using the upper extremity.

NHP models can be appropriately used to evaluate the safety of a candidate treatment. In these experiments, combination treatment with TRH, selenium, and Vitamin E did not result in any adverse side effects. In addition, the post mortem examinations did not demonstrate any evidence of toxicity. As a general construct, demonstrating safety in an NHP model is reassuring, when proposing to administer a candidate treatment in human beings. In this context, combination treatment is probably safe to offer in human clinical trials.

In human clinical practice, CNS lesions can affect the dominant and nondominant limbs asymmetrically. In addition, this clinical observation of limb preference is recognized in NHP.[25,32] As such, the physiologic and functional consequences of a CNS lesion may have disparate effects on the dominant and nondominant sides of the body.

The statistical power in these experiments in enhanced by the collection of EMG data prior to the creation of a lesion. This practice permits normalization of the postlesion data for each subject, theoretically decreasing statistical variances. In addition, the prelesion and postlesion data were collected daily basis, such that each recording date serves as a unique data point, thus permitting inferences regarding the trajectory of recovery. Therefore, our current experimental strategy decreases the number of subjects required to ascertain a treatment effect.

Given the EMG data from these experiments, Q can be used to evaluate impairment after TSCI. Specifically, Q is decreased immediately after experimental TSCI and increases over time. However, evidence is insufficient to ascribe a treatment-associated effect. Regardless, the results from these experiments have provided insights into statistical variances of Q and will serve as a guide for future experiments.

The rationale for the combination therapy in TSCI in general and regarding the TRH–selenium–vitamin E combination specifically is published elsewhere.[39] One of the goals of the current experiments was to gain a preliminary understanding of the safety and efficacy of the combination of these 3 agents, which had not previously been evaluated in animal models or human studies. In a clinical trial involving human patients who experienced TSCI, TRH was administered as a 0.2-mg/kg bolus followed by infusion of 0.2 mg/kg/h for 6 h.[33] For the current study, a similar weight-based dosing paradigm was used: macaques in the treatment group received a bolus of 0.2 mg/kg with continued infusion of 0.2 mg/kg/h for 1 h while anesthetized. Although the infusion could have been maintained for a longer period of time, doing so might have increased the risk of adverse effects related to anesthesia. In addition, selenium and vitamin E are antioxidants and thus might mitigate the pathophysiology of TSCI.[3,36,41] In selecting the doses for these initial experiments, we considered the human clinical experience. In the context of the weight of the macaques, we reduced the selenium and vitamin E doses to 20% of reasonable doses in humans. For example, patients in the SELECT trial received

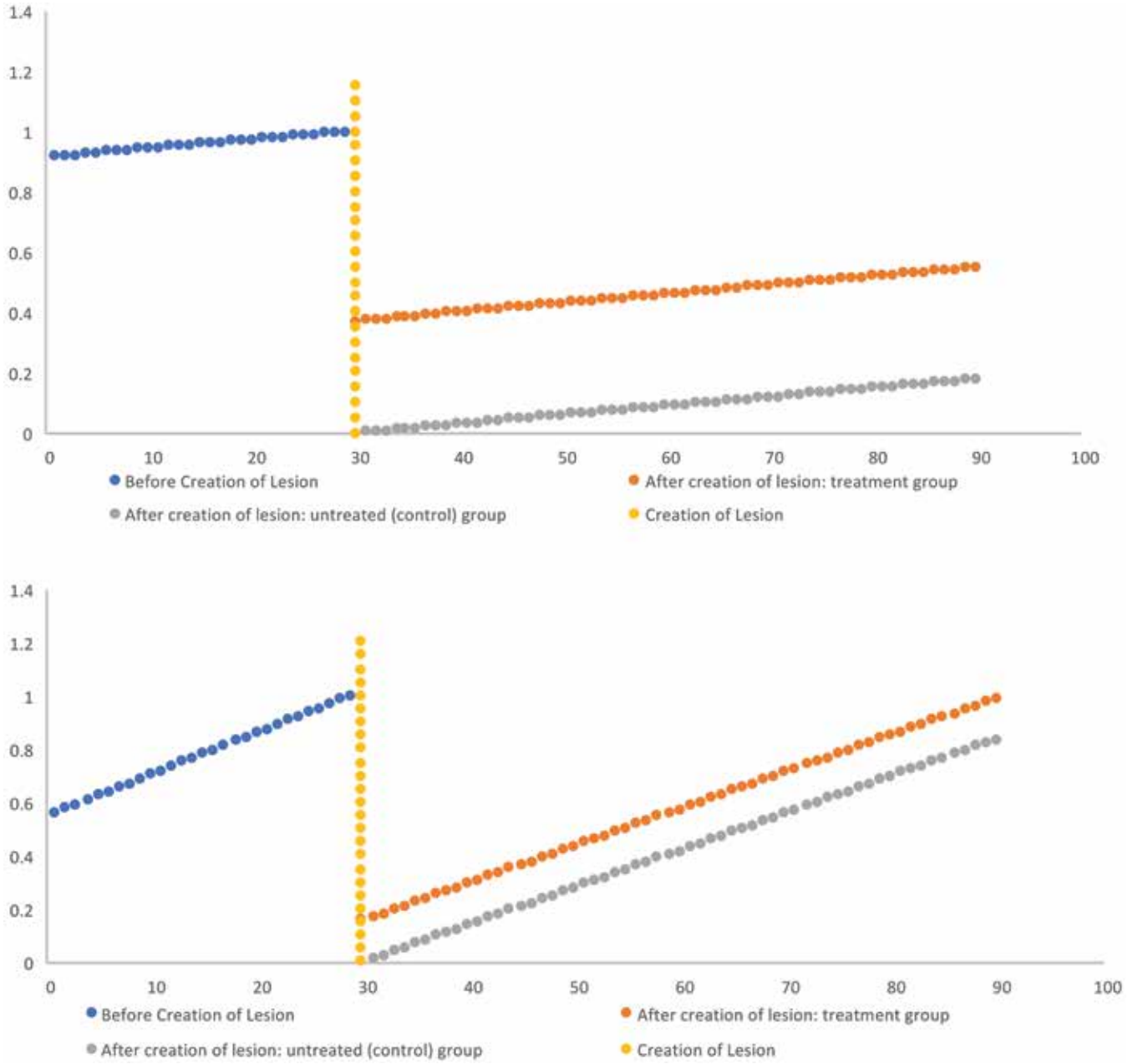


**Figure 9.** The aggregate fitted Q-values, representing tail movement, are plotted over 90 d for the left (top) and right (bottom) sides. Values are normalized to range between 0 to 1, with higher values indicating greater muscle activity. Of note, in both the left and right side, Q values are decreased immediately after creation of the lesion. On the left side, the effect of the lesion in the treatment group (orange) was attenuated, compared with the nontreatment group (grey). On both the left and right sides, Q scores improved over time.

200 mg of selenium and 400 IU of vitamin E.[21] However, the US Office of Dietary Supplements has stated that a selenium dose of 400 mg daily is safe.[26] As a compromise, for the current study, we chose a selenium dose target of 300 mg; dividing the target doses by 5 results in administered doses of 60 mg of selenium and 80 IU of vitamin E.

The histopathologic data revealing the presence of macrophages and microglia suggest that the inflammatory process continues at 90 d after creation of the TSCI lesion. Furthermore inflammation was present at the site of injury and both rostrally and caudally. We speculative that this continued inflammatory cascade might be modulated by biologic agents such as natalizumab, alemtuzumab, mitoxantrone, and ocrelizumab, which are currently used to treat neuroinflammation in patients with multiple sclerosis.[10,40]

A single animal model cannot entirely recapitulate the human experience. Although the histopathologic findings from our macaque model are similar to those in human TSCI, our model is particularly relevant to injuries associated with solid-core lesions. In addition, we qualitatively evaluated the spinal cord specimens. In the future, qualitative approaches might provide additional inferences.

Several potential alternative approaches to analyzing the EMG data are available. The EMG analysis paradigm that we used in the current study focused on the number of peaks in the EMG continuous signal. An alternative approach is to evaluate the data with the assumption that greater EMG activity

translates to greater recruitment of motor units. Operationally, the aggregate EMG signal could be 'decomposed' into single or groups of motor units. Another approach is to consider the nature of the EMG signal at the point of change in movement of the tail. This method would involve evaluating the periods of cocontractions between the agonist and antagonist muscles; some evidence indicates that cocontraction is a clinical phenomenon in human TSCI. In addition, video images of tail movement might be obtained concurrently with the EMG data, and this information might be incorporated into the analysis paradigm. Despite the technical challenges, this area merits further refinement and potential research.

In conclusion, the EMG and histopathologic data from this study advances our understanding of TSCI. The additional research required may translate into novel treatments for people and animals with spinal cord injury.

## Acknowledgments

This work was presented in part as a poster at the 2016 Annual Meeting of the American Association of Neuropathologists.

Research reported in this publication was supported in part by the Office of The Director, National Institutes of Health, under Award Number P51OD011106 to the Wisconsin National Primate Research Center, University of Wisconsin-Madison. This research was conducted in part at a facility constructed with support from Research Facilities Improvement Program grant numbers RR15459-01 and RR020141-01. The New England Primate Research Center was the recipient of NIH Grant 5P51RR000168. The content is solely the responsibility of the authors and does not necessarily represent the official views of the National Institutes of Health.

## References

1. **Algotar AM, Stratton MS, Ahmann FR, Ranger-Moore J, Nagle RB, Thompson PA, Slate E, Hsu CH, Dalkin BL, Sindhwani P, Holmes MA, Tuckey JA, Graham DL, Parnes HL, Clark LC, Stratton SP.** 2012. Phase 3 clinical trial investigating the effect of selenium supplementation in men at high-risk for prostate cancer. Prostate **75:**328–335.
2. **Allen AR.** 1911. Surgery of experimental lesion of spinal cord equivalent to crush injury of fracture dislocation of spinal column. JAMA **LVII:**878–880.
3. **Anderson DK, Saunders RD, Demediuk P, Dugan LL, Braughler JM, Hall ED, Means ED, Horrocks LA.** 1985. Lipid hydrolysis and peroxidation in injured spinal cord: partial protection with methylprednisolone or vitamin E and selenium. Cent Nerv Syst Trauma **2:**257–267.
4. **Beattie MS, Bresnahan JC, Komon J, Tovar CA, VanMeter M, Anderson DK, Faden AL, Hsu CY, Noble LJ, Salzman S, Young W.** 1997. Endogenous repair after spinal cord contusion injuries in the rat. Exp Neurol **148:**453–463.
5. **Brown TG.** 1911. The intrinsic factors in the act of progression in the mammal. Proc R Soc Lond B Biol Sci **84:**308–319.
6. **Bunge RP, Puckett WR, Becerra JL, Marcillo A, Quencer RM.** 1993. Observations on the pathology of human spinal cord injury. A review and classification of 22 new cases with details from a case of chronic cord compression with extensive focal demyelination. Adv Neurol **59:**75–89.
7. **Capogrosso M, Milekovic T, Borton D, Wagner F, Moraud EM, Mignardot JB, Buse N, Gandar J, Barraud Q, Xing D, Rey E.** 2016. A brain–spine interface alleviating gait deficits after spinal cord injury in primates. Nature **539:**284–288.
8. **Chamberlain JD, Meier S, Mader L, von Groote PM, Brinkhof MW.** 2015. Mortality and longevity after a spinal cord injury: a systematic review and meta-analysis. Neuroepidemiology **44:**182–198. PubMed
9. **Chang HT.** 2007. Subacute human spinal cord contusion: few lymphocytes and many macrophages. Spinal Cord **45:**174–182.
10. **Dargahi N, Katsara M, Tselios T, Androutsou ME, de Courten M, Matsoukas J, Apostolopoulos V**. 2017. Multiple sclerosis: immunopathology and treatment update. Brain Sci **7:** 1–27.
11. **Eidelberg E, Story JL, Meyer BL, Nystel J.** 1980. Stepping by chronic spinal cats. Exp Brain Res **40:**241–246.
12. **Eidelberg E, Walden JG, Nguyen LH.** 1981. Locomotors control in macaque monkeys. Brain **104:**647–663.
13. **Faden AI.** 1989. TRH analog YM-14673 improves outcome following traumatic brain and spinal cord injury in rats: dose-response studies. Brain Res **486:**228–235.
14. **Faden AI.** 1996. Pharmacological treatment of central nervous system trauma. Pharmacol Toxicol **78:**12–17.
15. **Fleming JC, Norenberg MD, Ramsay DA, Dekaban GA, Marcillo AE, Saenz AD, Pasquale-Styles M, Dietrich WD, Weaver LC.** 2006. The cellular inflammatory response in human spinal cords after injury. Brain **129:**3249–3269.
16. **Fulton JF, Sherrington CS.** 1932. State of the flexor reflex in paraplegic dog and monkey respectively. J Physiol **75:**17–22.
17. **Goossens ME, Buntinx F, Joniau S, Ackaert K, Ameye F, Billiet I, Braeckman J, Breugelmans A, Darras J, Dilen K, Goeman L, Kellen E, Tombal B, Van Bruwaene S, Van Cleyenbreuge B, Van der Aa F, Vekemans K, Van Poppel H, Zeegers MP.** 2012. Designing the selenium and bladder cancer trial (SELEBLAT), a phase lll randomized chemoprvention study with selenium on recurrence of bladder cancer in Belgium. BMC Urol **12:**8.
18. **Graham WA, Rosene DL, Westmoreland S, Miller A, Sejdic E, Nesathurai S.** 2013. Humane nonhuman primate model of traumatic spinal cord injury utilizing electromyography as a measure of impairment and recovery. Open J Vet Med **3:**86–89.
19. **Grand TI.** 1972. A mechanical interpretation of terminal branch feeding. J Mammal **53:**198–201.
20. **Institute for Laboratory Animal Research.** 2011. Guide for the care and use of laboratory animals. Washington (DC): National Academic Press.
21. **Klein EA, Thompson IM Jr, Tangen CM, Crowley JJ, Lucia MS, Goodman PJ, Minasian LM, Ford LG, Parnes HL, Gaziano JM, Karp DD, Lieber MM, Walther PJ, Koltz L, Parsons JK, Chin JL, Darke AK, Lippman SM, Goodman GE, Meyskens FL Jr, Baker LH.** 2011. Vitamin E and the risk of prostate cancer: the Selenium and Vitamin E cancer prevention trial (SELECT). JAMA 306:1549–1556.
22. **Love S, Louis DN, Ellison DW, editors.** 2008. Greenfield's neuropathology, 8th ed. London (United Kingdom): Hodder Arnold.
23. **Ma Z, Zhang YP, Liu W, Yan G, Li Y, Shields LBE, Walker M, Chen K, Huang W, Kong M, Lu Y, Brommer B, Chen X, Xu XM, Shields CB.** 2016. A controlled spinal cord contusion for the rhesus macaque monkey. Exp Neurol **279:**261–273.
24. **McKay WB, Ovechkin AV, Vitaz TW, Terson de Paleville DG, Harkema SJ.** 2011. Neurophysiological characterization of motor recovery in acute spinal cord injury. Spinal Cord **49:**421–429.
25. **Meguerditchian A, Phillips KA, Chapelain A, Mahovetz LM, Milne S, Stoinski T, Bania A, Lonsdorf E, Schaeffer J, Russell J, Hopkins WD.** 2015. Handedness for unimanual grasping in 564 great apes: the effect on grip morphology and a comparison with hand use for a bimanual coordinated task. Front Psychol **6**:1–9.
26. **National Institutes of Health.** [Internet]. 2016. Selenium dietary supplement fact sheet. Office of Dietary Supplements. [Cited 14 November 2017]. Available at: https://ods.od.nih.gov/factsheets/Selenium-HealthProfessional/
27. **Nesathurai S.** 2013. The rehabilitation of people with spinal cord injury, 3rd ed. Whitinsville (MA):Arbuckle Academic Publishers.
28. **Nesathurai S, Graham WA, Mansfield K, Magill D, Sehgal P, Westmoreland SV, Prusty S, Rosene DL, Sledge JB.** 2006. Model of traumatic spinal cord injury in *Macaca fascicularis*: similarity of experimental lesions created by epidural catheter to human spinal cord injury. J Med Primatol **35:**401–404.
29. **Nesathurai S, Andrew Graham W, Edell DJ, Rosene DL, Mansfield K, Sehgal P, Magill D, Sledge JB.** 2006. Electromyographic telemetry in the development of humane primate model of spinal cord injury. J Med Primatol **35:**397–400.
30. **Norreel JC, Pflieger JF, Pearlstein E, Simeoni-Alias J, Clarac F, Vinay L.** 2003. Reversible disorganization of the locomotor

pattern after neonatal spinal cord transection in the rat. J Neurosci **23:**1924–1932.

31. **Nout YS, Rosenzweig ES, Brock JH, Strand SC, Moseanko R, Hawbecker S, Zdunowski S, Nielson JL, Roy RR, Courtine G, Ferguson AR, Edgerton VR, Beattie MS, Bresnahan JC, Tuszynski MH.** 2012. Animal models of neurologic disorders: a nonhuman primate model of spinal cord injury. Neurotherapeutics **9:**380–392.
32. **Ojha PR.** 1974. Tail carriage and dominance in the rhesus monkey *Macaca mulatta*. Mammalia **38:**163–170.
33. **Pitts LH, Ross A, Chase GA, Faden AI.** 1995. Treatment with thyrotropin-releasing hormone (TRH) in patients with traumatic spinal cord injuries. J Neurotrauma **12:**235–243.
34. **Rivlin AS, Tator CH.** 1978. Effect of duration of acute spinal cord compression in a new acute cord injury model in the rat. Surg Neurol **10:**38–43.
35. **Rodman PS.** 1979. Skeletal differentiation of *Macaca fascicularis* and *Macaca nemestrina* in relation to arboreal and terrestrial quadrupedalism. Am J Phys Anthropol **51:**51–62.
36. **Saunders RD, Dugan LL, Demediuk P, Means ED, Horrocks LA, Anderson DK.** 1987. Effects of methylprednisolone and the combination of α-tocopherol and selenium on arachidonic acid metabolism and lipid peroxidation in traumatized spinal cord tissue. J Neurochem **49:**24–31.
37. **Seth N, Masood F, Sledge J, Graham W, Rosene D, Westmoreland S, Macri S, Sejdic E, Hoggatt A, Simmons H, Abdullah H, Nesathurai S.** 2015. Humane nonhuman primate model of traumatic spinal cord injury: quantitative analysis of electromyographic data. Open J Vet Med **5:**161–168.
38. **Sledge J, Graham WA, Westmoreland S, Sejdic E, Miller A, Hoggatt A, Nesathurai S.** 2013. Spinal cord injury models in nonhuman primates: are lesions created by sharp instruments relevant to human injuries? Med Hypotheses **81:**747–748.
39. **Sledge J, Mahadevappa K, Stacey P, Graham A, Nesathurai S.** 2016. A speculative pharmaceutical cocktail to treat spinal cord injury. Am J Phys Med Rehabil **95:**e108–e110.
40. **Torkildsen O, Myhr KM, Bo L.** 2015. Disease-modifying treatments for multiple sclerosis – a review of approved medications. Eur J Neurol **23 Suppl 1:**18–27.
41. **Yeo JE, Kim JH, Kang SK.**2008. Selenium attenuates ros-mediated apoptotic cell death of injured spinal cord through prevention of mitochondria dysfunction; in vitro and in vivo study. Cell Physiol Biochem **21:**225–238.
42. **Yusuf S, Dagenais G, Pogue J, Bosch J, Sleight P.** 2000. Vitamin E supplementation and cardiovascular events in high-risk patients. N Engl J Med **342:**154–160.